Molecular Crystals and Liquid Crystals
Publication details, including instructions for authors and subscription information:
http://www.tandfonline.com/loi/gmcl16

The Influence of an External Electric Field on the Structure of Chiral Sm C* Liquid Crystal

M. Glogarová [a] , L. Lejček [a] , J. Pavel [a] , V. Janovec [a] & J. Fousek [a]

[a] Institute of Physics, Czech. Acad. Sci., Na Slovance 2 180 40, Prague, 8, Czechoslovakia

To cite this article: M. Glogarová , L. Lejček , J. Pavel , V. Janovec & J. Fousek (1983): The Influence of an External Electric Field on the Structure of Chiral Sm C* Liquid Crystal, Molecular Crystals and Liquid Crystals, 91:3-4, 309-325

To link to this article: http://dx.doi.org/10.1080/00268948308083692

Mol. Cryst. Liq. Cryst., 1983, Vol. 91, pp. 309–325
0026-8941/83/9104–0309/$18.50/0

The Influence of an External Electric Field on the Structure of Chiral Sm C* Liquid Crystal

M. GLOGAROVÁ, L. LEJČEK, J. PAVEL, V. JANOVEC and J. FOUSEK

*Institute of Physics, Czech. Acad. Sci., Na Slovance 2, 180 40
Prague 8, Czechoslovakia*

(Received September 2, 1982; in final form November 5, 1982)

The mechanism of a field induced transition from helical Sm C* to Sm C structure in a DOBAMBC liquid crystal situated between two glass plates has been studied by optical methods. The important role of a regular system of twist disclination lines (dechiralization lines) in unwinding the helical structure by electric field has been revealed. A simplified model of $\pm 2\pi$ twist disclination pairs is proposed which describes the unwinding of the Sm C* structure. Under the external electric field the pairs of $\pm 2\pi$ twist disclinations move and annihilate each other and thus effectively unwind the helical structure of the sample. Critical fields for switching the helical Sm C* structure, as well as the unwound structure, are estimated.

1 INTRODUCTION

In chiral Sm C (Sm C*) liquid crystal structure the long molecules are arranged in layers and tilted by an angle θ with respect to the layer normal. The chirality of a molecule results in a helical structure of tilted molecules when going from layer to layer in the normal direction.[1] The molecules precess by the angle 2π over the pitch of the spiral structure p_0. The chirality of molecule is coupled to the electric dipole moment which can interact directly with the external electric field.

The first experimental evidence of the influence of an external electric field upon the chiral smectic helix was based on the observation of conoscopic image.[1] The change of uniaxial conoscopic image to a biaxial one under the electric field parallel to the smectic layers was attributed to switching from Sm C* to Sm C structure. Two different orientations of Sm C corresponded to antiparallel electric fields.[1] A polarization response during the switching process showed a similar hysteresis as for crystalline ferroelectrics.[2-4] Direct observation of the Sm C* texture in a plate-like cell revealed a system of dark and light stripes with a periodical distance of about 3 μm.[2,5-8] The stripes were ascribed to linear defects situated near the sample surface and spaced at the distance p_0 from each other,[9-11] or they were explained as an optical consequence of a regular spiral structure.[2,5,7,8] If alternating fields of about 50 Hz were applied with increasing amplitude, the distance between the stripes gradually increased. For a critical field amplitude the stripes disappeared.[6,12] Till now no attention has been paid to the behavior of the stripes in intermediate d.c. fields. All theoretical treatments of the interaction of an electric field with Sm C* (see *e.g.*[13-17]) published by now, assumed an infinite sample. The transition Sm C* → Sm C induced by a critical electric field was interpreted as the unwinding of the smectic helix. The unwinding mechanism in samples of finite thickness has not yet been considered.

In this paper our observations of the interaction of an external d.c. electric field with *p*-*n*-decyloxybenzilidene-*p*′-amino 2 methyl butyl cinnamate (DOBAMBC) chiral smectic liquid crystal sample are presented and a simplified model of the process of unwinding the Sm C* helix in finite samples is proposed. Preliminary results have been reported.[18]

2 EXPERIMENTAL RESULTS

The DOBAMBC liquid crystal heated to its isotropic phase was filled between two glass plates by capillary suction. Mylar spacers 20, 30, and 50 μm thick were used to define the sample thickness. The glass plates coated by thin SnO_2 layers served as electrodes.

We have studied both non-oriented samples and samples oriented in a magnetic field applied in the plane of the sample. The magnetic field of about 1,5 T was applied for two hours at cooling from the isotropic phase (from about 120°C) through Sm A phase (temperature range 117°–95°C) to Sm C* phase. Then the samples were investigated in polarizing microscope without magnetic field.

In the sample aligned in transversal magnetic field the smectic layers are mostly perpendicular to both the sample plane and the magnetic field direction. Sometimes very long focal conics remain, which can be partially expelled by electric field of 100 Hz, 10 kV/cm applied for several minutes. In Sm C* phase a system of parallel lines appears which is seen even in unpolarized light. However, the best optical contrast is obtained in crossed polarizers (Figure 1a). When the sample is rotated between crossed polarizers no lateral shift of the lines is observed. The distance between the lines is about 2,5 μm and does not change significantly with temperature.

If a d.c. electric field is applied, no continuous changes of the line distance are observed up to the field intensity of about 3 kV/cm. For higher fields, the lines become successively shorter and eventually disappear (Figures 1b, c). During this process the periodicity of the line structure is lost. When the field is switched off line nuclei appear, usually within seconds lengthen through the whole sample, and thus the periodical line structure is recovered again. Sometimes when only few separated lines are present, they appear doubled (Figure 1c). By changing the microscope focusing we have found that the doubled lines are, in fact, thin loops with long linear parts located near upper and lower glass plates. The plane of the loop is nearly perpendicular to the sample plane. For the field intensity slightly above 3 kV/cm all the lines or loops disappear and the whole sample is homogeneously bright or dark depending on the field polarity. The angular difference of optical extinction position for two antiparallel electric fields is about 44 deg. at temperatures about 3° below the Sm A → Sm C* phase transition.

After repeated switching of the d.c. field polarity, the system of lines does not appear immediately when the field is switched off. Several seconds are needed to recover the line pattern. If the field of opposite polarity

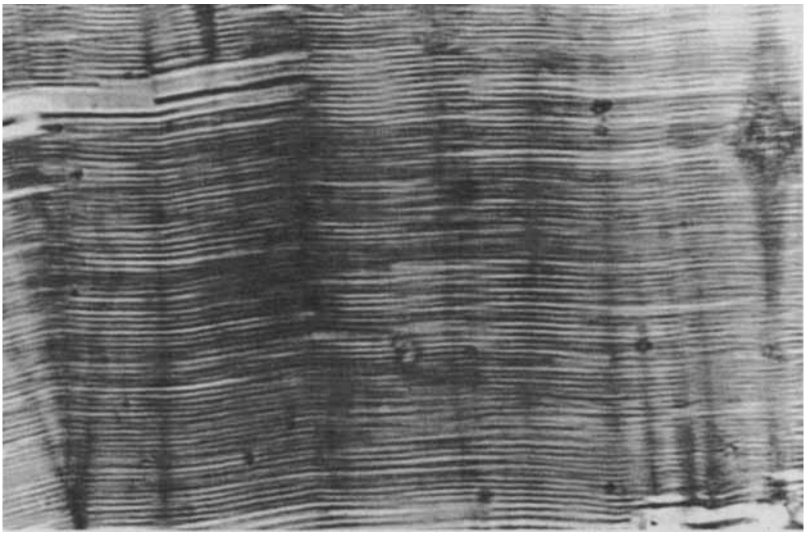

(*a*)

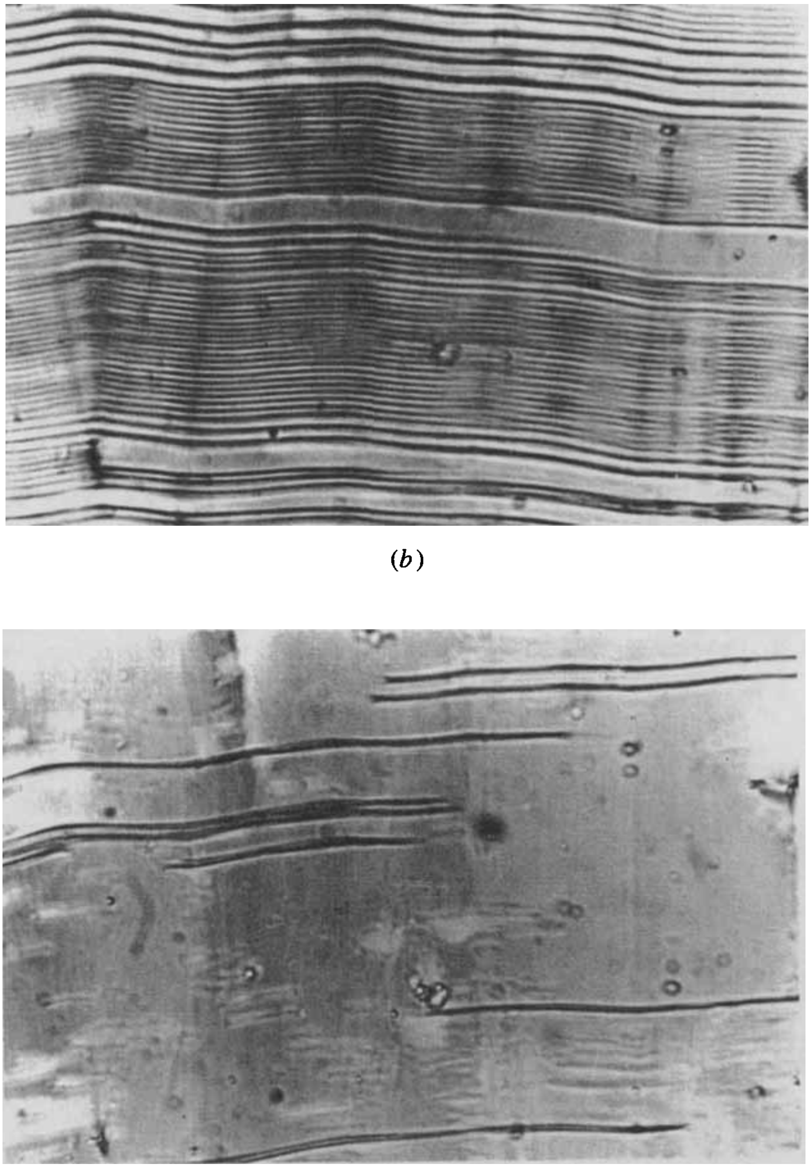
(*b*)

(*c*)

FIGURE 1 A texture of Sm C* DOBAMBC sample 50 μm thick oriented in magnetic field. Dimensions of the surface region are (0,37 × 0,25) mm^2; a) $E = 0$, *b*, *c*) d.c. field $E = 3kV/cm$, dechiralization lines disappear gradually within a few seconds; c) Doubling of lines is seen.

is applied before that, the areas of the other orientation arise in a form of irregular islets, which grow with increasing field intensity (Figures 2a, b). The islets are elongated in the direction parallel to the smectic layers.

With non-oriented samples the focal conic texture appearing in Sm A phase undergoes no changes after cooling to Sm C* phase. At the Sm A → Sm C* phase transition temperature a system of lines with the period of about 2,5 μm appears (Figure 3). With the samples 50 μm thick the focal conic texture near the upper glass plate differs from that near the lower one. The systems of lines near the upper and lower glass plates differ significantly tracing the smectic layers belonging to a certain focal conic.

When a d.c. field is applied, the distances between lines do not change up to the intensity of about 3 kV/cm. At higher intensities the lines successively disappear starting from the boundaries of focal conics (Figure 4). For the field slightly higher than 3 kV/cm the field induced phase transition Sm C* → Sm C is completed.

3 INTERPRETATION OF THE OBSERVED RESULTS

The optical observations just described indicate that the lines, which appear in Sm C* phase are not the direct optical consequence of the spiral structure as previously suggested[5,8] and assumed.[2,7,12] If the sample is observed between crossed polarizers the continuous change of the director along the helical axis of Sm C* should result in a continuous change of optical contrast along this axis. Moreover, the stripes of maximum and minimum light intensities should exhibit a sidewise shift when the sample is rotated between crossed polarizers,[5] or the stripes should be focused out of the sample.[8] Instead of diffused lines we observed sharp lines typical for linear defects which were seen even in unpolarized light. When the sample was rotated between crossed polarizers, no lateral shift of lines was observed.

In accordance with[9-11] we suppose that the regular lines which are seen in Sm C* phase correspond to linear defects. These defects, called dechiralization lines, mediate the unwound Sm C* which arises near the glass plate due to the planar anchoring on the plates, and helical Sm C* in the bulk of the sample. A sharp optical contrast connected with the dechiralization lines probably suppresses the optical contrast due to the spiral structure, which should appear as continuous changing dark and bright stripes parallel to the disclination lines.

A topological model of the structure of Sm C* around dechiralization lines was proposed[9] for the smectic layers perpendicular to the sample plane. From this model it follows that the lines form pairs of $\pm 2\pi$ twist disclinations situated near the upper and lower glass plates, respectively,

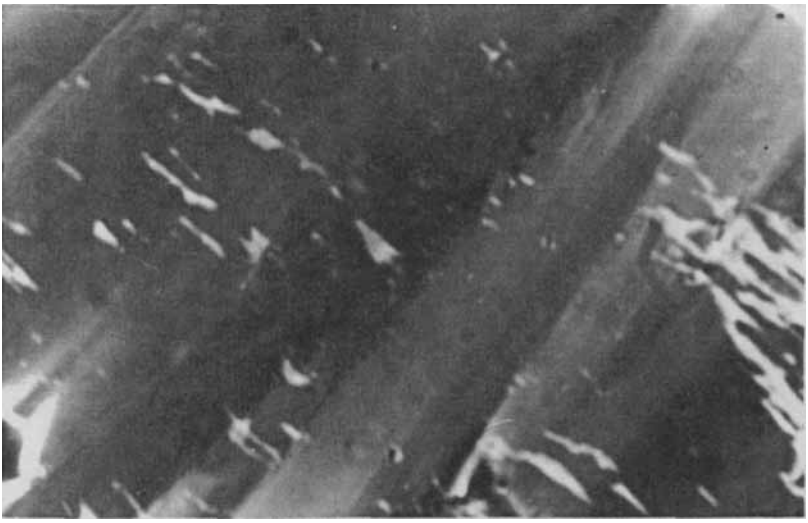

(*a*)

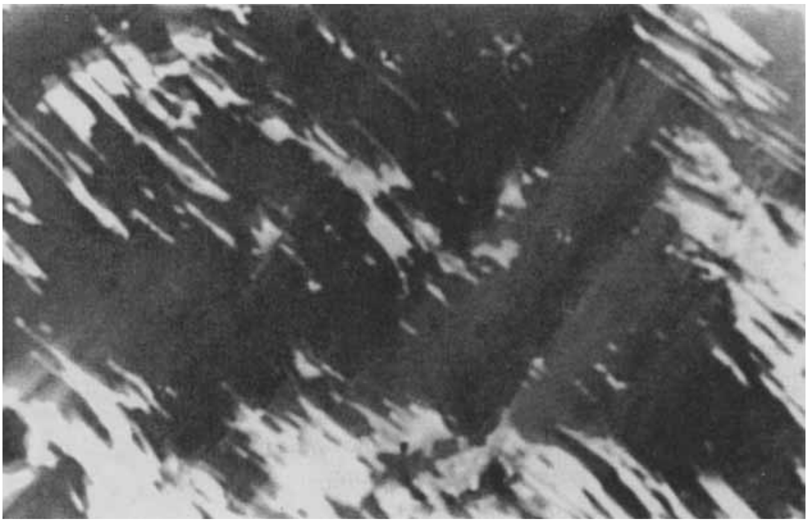

(*b*)

FIGURE 2 a,b) Two different intermediate stages at switching of DOBAMBC oriented sample 50 μm thick in a d.c. field of 3kV/cm. The new orientation appears as bright areas. Dimensions of the surface region are (0,37 × 0,25) mm^2.

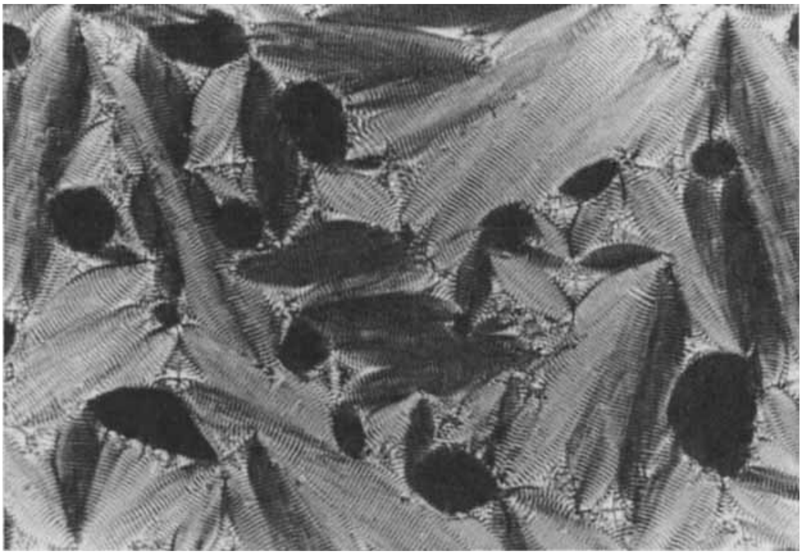

FIGURE 3 A fan-shaped texture with dechiralization lines in DOBAMBC non-oriented sample 30 μm thick in Sm C* phase as seen between crossed polarizers. The black areas are air bubbles. The area of the figure is (0,37 × 0,25) mm^2.

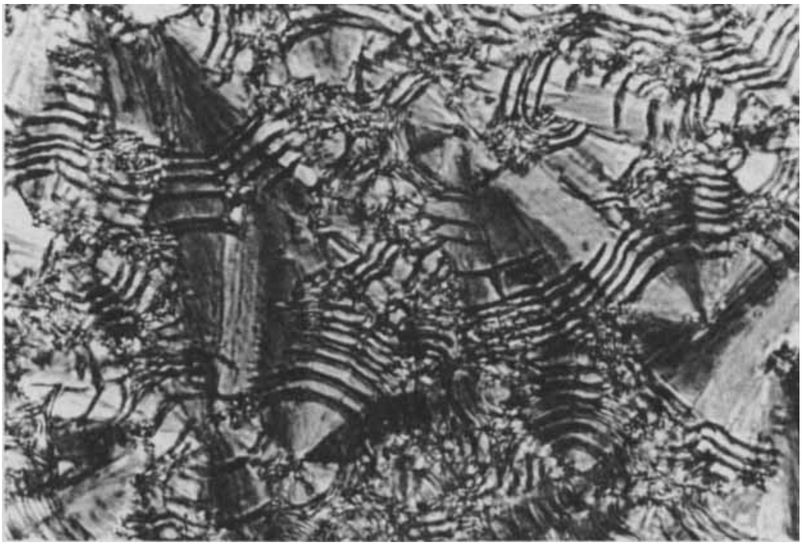

FIGURE 4 A texture of Sm C* DOBAMBC non-oriented sample 50 μm thick just after d.c. field $E = 3\text{kV/cm}$ has been applied. Remaining dechiralization lines are seen. The area of the figure is (0,37 × 0,25) mm^2.

parallel to the sample plane and to the smectic layers. The distance between the lines near the same glass plate equals the helical pitch. The pair of $\pm 2\pi$ twist disclinations is situated in the same smectic layer so that in perfectly oriented samples they lie one over the other, and so they cannot be resolved optically.

In our opinion, if a d.c. electric field is applied the $\pm 2\pi$ lines of the same smectic layer close upon themselves at the side ends of the sample or at some defects, creating thus, a long loop which becomes shorter under the field. The loops are observable only when the smectic layers are not strictly perpendicular to the sample plane, then $+2\pi$ and -2π twist disclinations do not superimpose. When $+2\pi$ and -2π lines meet they annihilate each other. The disappearance of one pair of $\pm 2\pi$ disclinations is equivalent to unwinding the helical structure by 2π. The annihilation of all pairs of $\pm 2\pi$ twist disclinations completely unwinds the helical structure.

We have observed the unwound structure even after removing the external electric field. The structure preserves homogeneous Sm C ordering for several seconds. These metastable samples (20–30 μm thick) exhibit bistable switching (see Figures 2a, b) similar to that observed in very thin samples where the structure was unwound due to the surface anchoring.[19]

With non-oriented samples the dechiralization lines follow the smectic layers on focal conics. For this case a model of the Sm C* structure around the lines was proposed.[11,28] Different patterns of sharp lines we have observed when focusing just below the upper and just above the lower glass plates could hardly be caused by contrast on the spiral structure in the bulk, whereas linear defects provide a consistent explanation.

4 DECHIRALIZATION LINES AND FIELD INDUCED Sm C* → Sm C TRANSITION—A SIMPLIFIED MODEL

In this part the solution describing the system of dechiralization lines will be derived (Section 4.2) using the free energy of Sm C* with nondeformed layers (Section 4.1). The behavior of these lines when external electric field is applied will be studied within the simplified model (Section 4.3)

4.1 Approximation of the free energy density

We start with the approximation of the free energy density. Supposing the smectic layers to be parallel, the elastic part of the free energy representing the energy increase with respect to the ideal Sm C* structure can be written in the form

$$f_{el} = \frac{B_1}{2}(\mathbf{t} \times \mathrm{rot}\ \mathbf{t})^2 + \frac{B_2}{2}(\mathrm{div}\ \mathbf{t})^2 + \frac{B_3}{2}(\mathbf{t}\ \mathrm{rot}\ \mathbf{t} + q_0)^2 \qquad (1)$$

similarly to.[20,25] The **t**-vector is a direction of the projection of molecules into smectic layer (**t**-vector was introduced e.g.,[20] see also Figure 5). B_1, B_2, and B_3 are the elastic constants and q_0 is related to the pitch of helical structure of Sm C* liquid crystal by the relation $p_0 = 2\pi/q_0$. For simplicity let us suppose that $B_1 = B_2$. If $\mathbf{t} = (0, \cos\phi, \sin\phi)$ where $\phi = \phi(x, z)$ is an angle between **t** and y-axis (Figure 5), the expression (1) can be transformed to

$$f_{el} = \frac{B_1}{2}\left(\frac{\partial\phi}{\partial z}\right)^2 + \frac{B_3}{2}\left(-\frac{\partial\phi}{\partial x} + q_0\right)^2. \tag{2}$$

The part of the free energy density which describes the interaction of smectic crystal with an external electric field **E** can be taken into account as in Ref. 21

$$f_E = \mu_1\chi \cos\theta \sin\theta(E_y t_z - E_z t_y). \tag{3}$$

Here the assumption is used that the flexoelectric term, $-\mu_2\chi \cos\theta \sin\theta$ $[E_y(\partial t_z/\partial x) + E_z(\partial t_y/\partial x)]$, does not play an important role, i.e., $\mu_1 \gg \mu_2$ and also the quadratic term in **E**, i.e., χE_z^2, will not be taken into the account. The constants μ_1 and μ_2 are the piezoelectric and flexoelectric constants; respectively, θ is the tilt angle a molecule makes with the x-axis which will be taken as constant throughout the whole sample and χ is dielectric susceptibility. We restrict our investigation to the case $E_z \neq 0$ and $E_y = 0$, i.e., the electric field is applied perpendicularly to the glass surfaces (Figure 5).

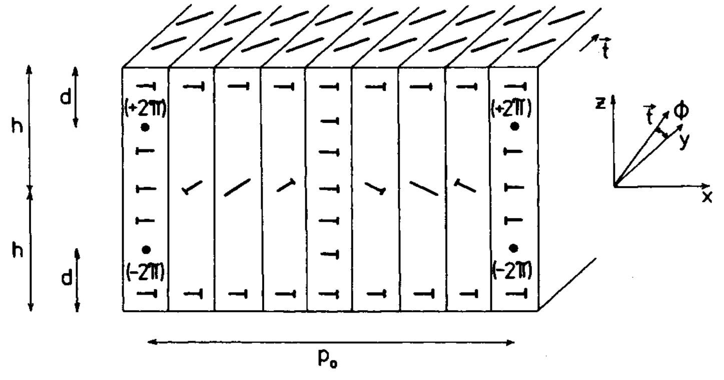

FIGURE 5 Coordinate axes and schematic representation of molecular arrangement around $\pm 2\pi$ dechiralization lines (dots with $\pm 2\pi$). The molecules are represented by nails[21] the points of which correspond to those parts of molecules which are turned toward the observer. **t**-vector is the projection of molecules into the plane of Sm C* layer, making an angle ϕ with y-axis. $2h$ is the sample thickness, d is the distance of lines from glass plates and p_0 designates the helical pitch.

The surface anchoring energy will be taken into account in the simple form[23] $W_s \sin^2 \phi_0$ where W_s is the maximum surface energy of anchoring. The angle of **t**-vector with the y-axis is ϕ_0.

Then the total energy F of the sample per unit length of y-axis, over the period p_0 and over the half thickness h is

$$F = \int_0^h dz \int_{-p_0/2}^{p_0/2} dx \left\{ \frac{B_1}{2}\left(\frac{\partial\phi}{\partial z}\right)^2 + \frac{B_3}{2}\left(-\frac{\partial\phi}{\partial x} + q_0\right)^2 - P_s E_z \cos\phi \right\} + \int_{-p_0/2}^{p_0/2} dx \left[W_s \sin^2\phi_0 \right]_{z=+h}; \qquad (4)$$

where $P_s = \mu_1 \chi \cos\theta \sin\theta$ is the local spontaneous polarization and $2h$ is the thickness of the sample.

4.2 Dechiralization lines

The experiments reviewed in Part 3, show that in the sample the system of $\pm 2\pi$ twist disclination lines exists. Now we will look for such a solution of the equation of equilibrium which describes the system of lines without an external electric field.

The variation of F in Eq. (4) with respect to ϕ and with $E_z = 0$ gives the equilibrium condition

$$B_1 \frac{\partial^2\phi}{\partial z^2} + B_3 \frac{\partial^2\phi}{\partial x^2} = 0 \qquad (5)$$

The boundary condition will be assumed in the form $\phi(z = \pm h) = \phi_0$ with ϕ_0 constant. We construct the solution of Eq. (5) corresponding to the periodical system of $\pm 2\pi$ twist disclination lines with period p_0 situated at the distances d from the upper and lower glass, respectively (see Figure 5). Using the function arctg $(\alpha z/x)$ as the elementary solution of Eq. (5) we finally obtain

$$\phi = \phi_0 + \sum_{n=-\infty}^{+\infty} \sum_{k=-\infty}^{+\infty} (-1)^k \left[\operatorname{arctg} \alpha \frac{z - 2hk - h + d}{x - np_0} - \operatorname{arctg} \alpha \frac{z - 2hk + h - d}{x - np_0} \right], \qquad (6)$$

where $\alpha = (B_3/B_1)^{1/2}$.

The solution (Eq. (6)) corresponds to the periodic distribution of pairs of $+2\pi$ and -2π twist disclinations situated at the points $[x = np_0, z = h - d]$ and $[x = np_0, z = -h + d]$, respectively. The mirror images of these disclination pairs with respect to the glass plates were added in order to satisfy the boundary conditions $\phi(z = \pm h) = \phi_0$ similarly, as in the case of dislocations in finite smectic crystal.[24]

The equilibrium distance d for $E_z = 0$ corresponds to a minimum of Eq. (4) with respect to d with ϕ given by Eq. (6) and ϕ_0 fixed. For the half-space of Sm C* crystal the similar problem was solved[10,25] by the different method used originally for cholesterics.[26]

For $z \in (-(h - d), (h - d))$ the angle ϕ changes by 2π at $x \to np_0$ and $\phi = \phi_0$ for $x = np_0/2$. So for h large and $z \to 0$ (i.e., in the middle of the sample) ϕ behaves as

$$\phi = \phi_0 + (2\pi/p_0)(x - p_0/2) \tag{7}$$

for $x \in (0, p_0)$. The ϕ as given by Eq. (6) is the periodic function of x with period p_0. Having the same form as Eq. (7) in each interval $x \in (np_0, (n + 1)p_0)$, $n = 0, \pm 1, \pm 2 \ldots$, it describes the ideal Sm C* structure.

The solution (Eq. (6)) represents both the perfect helical structure in the middle of a thick Sm C* sample and the system of pairs of $\pm 2\pi$ twist disclinations conjoining Sm C near the glass plates with Sm C* in the bulk of the sample.

Using the solution (Eq. (6)) which can be rewritten in the form

$$\begin{aligned}\phi = \phi_0 + \sum_{n=-\infty}^{+\infty} \{&\operatorname{arctg}[cth\pi Y_n tg\pi(Z - D_1)] - \operatorname{arctg}[cth\pi Y_n tg\pi(Z + D_1)] \\ &- \operatorname{arctg}[cth\pi Y_n tg\pi(Z + D_2)] + \operatorname{arctg}[cth\pi Y_n tg\pi(Z - D_2)]\}\end{aligned} \tag{8}$$

with $Y_n = (x - np_0)/4\alpha h$, $Z = z/4h$, $D_1 = (1 - d/h)/4$ and $D_2 = (1 + d/h)/4$, the equilibrium conditions for the system of the dechiralization lines can be found by the method described in Ref. 23. Introducing the torques

$$C_{xx} = \frac{\partial f_{el}}{\partial\left(\dfrac{\partial\phi}{\partial x}\right)} = B_3\left(\frac{\partial\phi}{\partial x} - q_0\right), \qquad C_{zx} = \frac{\partial f_{el}}{\partial\left(\dfrac{\partial\phi}{\partial z}\right)} = B_1\left(\frac{\partial\phi}{\partial z}\right), \tag{9}$$

the force g acting on a unit length of the disclination situated at $x = 0$, $z = (d - h)$ by the other disclinations is given by the expression analogous to Peach-Koehler equation[23] and has components

$$g_x = -2\pi C'_{zx}, \qquad g_y = 0, \qquad g_z = 2\pi C'_{xx}. \tag{10}$$

C'_{xx} and C'_{zx} follow from Eqs. (9) and (8) when the disclination at $x = 0$, $z = (d - h)$ is not included in the summation. The component $g_x = 0$, as a result of summation of equal values with opposite sign of force components in x-direction from the rest of disclinations. The component g_z is

$$g_z = \frac{\pi^2(B_1B_3)^{1/2}}{h}\sin\frac{\pi d}{h}\sum_{n=-\infty}^{+\infty}\left(\frac{ch2\pi Y_n}{ch^2 2\pi Y_n - \cos^2\pi\frac{d}{h}}\right)_{x=0} - p_0B_3q_0^2. \quad (11)$$

So in the sample without an external electric field the distance d of disclinations from the glass plates can be determined from the condition $g_z = 0$. In the special case when only the interaction of the nearest $+2\pi$ and -2π disclinations is considered, i.e., $h\alpha/p_0 < \pi/2$, the only term in Eq. (11) corresponding to $n = 0$ is taken into account. Then we obtain

$$\sin\frac{\pi d}{h} = \frac{p_0}{4h\alpha} \quad (12)$$

The Eq. (12) has for $h \geqslant p_0/4\alpha$ two solutions

$$d_1 = \frac{h}{\pi}\arcsin\frac{p_0}{4h\alpha}, \qquad d_1 < h/2; \qquad d_2 = h - d_1 \quad (13)$$

Let us denote $F(d)$ the part of F given in Eq. (4) which depends on d at the condition $E_z = 0$. The energy $F(d)$ is calculated over the volume containing one disclination. The force g_z acting on the unit length of the disclination can be expresed as $g_z = -\partial F(d)/\partial d$.

Then $\partial^2F(d)/\partial d^2 = -\partial g_z/\partial d$ is positive for $d = d_1$ and negative for $d = d_2$. Thus the solution $d = d_1$ describes the stable configuration of the disclination system. For a thick sample, i.e., h $\gg p_0$, it is $d_1 \approx p_0/4\pi\alpha$ which does not depend on h. In a thin sample where $h < p_0/4\alpha$, there are no dechiralization lines and all Sm C* liquid crystal is unwound due to the surface anchoring effect.[19]

4.3 The influence of an external electric field on Sm C*

When $E_z \neq 0$ the variation of Eq. (4) with respect to ϕ leads to the elliptic sine-Gordon equation in two dimensions.[27] However, in this paper we restrict our discussion to the simplified case in which

(i) the changes of ϕ around the disclination lines due to E_z and also the changes of pitch p_0 are neglected;

(ii) the Sm C* liquid crystal is unwound near glass plates up to the distance $2d$ and in the interval $z\epsilon(-(h - 2d), (h - 2d))$ the Sm C* sample has perfect helical structure. Then the term in Eq. (4)

$$F_E = -P_sE_z\int_0^h dz\int_{-p_0/2}^{p_0/2} dx\cos\phi$$

is approximated as $F_E = -2\,dp_0P_sE_z\cos\phi_0$;

(iii) only the interaction of the nearest $+2\pi$ and -2π disclinations is considered, i.e., the relation $h\alpha/p_0 < \pi/2$ is valid.

Then Eq. (4) yields

$$F = F_0 + F(d) - 2dp_0P_sE_z \cos \phi_0 + p_0W_s \sin^2 \phi_0 , \tag{14}$$

where F_0 is the part of F which depends neither on d nor on ϕ. The conditions of extreme with respect to the angle ϕ_0 and to the distance d lead to the equations

$$P_sE_zd \sin \phi_0 + W_s \sin \phi_0 \cos \phi_0 = 0 , \tag{15}$$

$$g_z = -2p_0P_sE_z \cos \phi_0 . \tag{16}$$

Eq. (15) yields

$$\phi_0 = 0, \pi , \tag{17}$$

$$\cos \phi_0 = -P_sE_zd/W_s \tag{18}$$

The solution Eq. (18) corresponds to the maximum of F with respect to the variable ϕ_0 and therefore will not be further considered.

The displacement $d(E)$ of the dechiralization lines under an applied field corresponding to the minimum of F with respect to d follows from Eq. (16)

$$d(E) = \frac{h}{\pi} \arcsin\left\{\pi^2(B_1B_3)^{1/2}/2p_0h\left(\frac{B_3}{2}q_0^2 - P_sE_z \cos \phi_0\right)\right\} \tag{19}$$

Suppose first that $\phi_0 = 0$ and $P_sE_z > 0$. By increasing E_z the distance $d(E)$ also increases, i.e., the disclinations move to the middle of the sample. For a critical field

$$|E_z^0| \approx \left[\frac{B_3}{2}q_0^2 - \frac{\pi^2(B_1B_3)^{1/2}}{2p_0h}\right] \Big/ |P_s| \tag{20}$$

we have $d(E_z^0) \approx h/2$. The system of $\pm 2\pi$ disclinations starts to be unstable for $d(E_z^0)$ and their attraction prevails. The disclinations move to the center of the sample and annihilate each other leaving the Sm C* sample unwound—the transition Sm C* → Sm C under the external field occurs. For a thick sample the second term in Eq. (20) is negligible, then $|E_z^0| \approx B_3q_0^2/2|P_s|$ as in Ref. 18.

When $\phi_0 = 0$ and $P_sE_z < 0$, the increase of E_z leads to the decrease of $d(E)$; however $d(E) \to 0$ for $|E_z| \to +\infty$, i.e., only an infinite field would shift the disclinations to the glass plates. So it is more probable that the molecules near glass surfaces change their orientation from $\phi_0 = 0$ to $\phi_0 = \pi$ under the influence of external field. For $\phi_0 = \pi$ and $P_sE_z < 0$ which is equivalent to $\phi_0 = 0$, $P_sE_z > 0$, disclinations again move to the center of the sample. In our model the switching mechanism of molecules in unwound Sm C* caused by a field is not incorporated. A few remarks on the possible mechanism of molecular reorientation will be given in the discussion.

Our approximation (assumption (i)) neglects a change of the spiral pitch. The dependence of the pitch p_0 on the electric field could be obtained as the solution of the equation $g_x = -(\partial F_E/\partial p_0)$. A more detailed study of this problem is in progress. In thin samples with $h < p_0/4\alpha$ the entire Sm C* liquid crystal is unwound due to the surface anchoring effect.[19] The critical field E_z^c to change the orientation in whole sample is the field which rotates molecules from the initial configuration $\phi_0 = 0$ to $\phi_0 = \pi/2$ corresponding to the maximum surface energy $2p_0W_s$. The electric energy needed to accomplish this process is $2p_0hP_sE_z^c$. Thus we obtain

$$E_z^c = W_s/hP_s \tag{21}$$

5 DISCUSSION AND CONCLUSIONS

In Section 3 we have shown that the lines seen in our samples of DOBAMBC in Sm C* phase are linear defects. The structure around the observed lines can be successfully described by topological model of disclination pairs first proposed for Sm C* liquid crystal in Ref. 9.

Similar defects were seen in cholesteric liquid crystal near the surface of the sample.[26] With cholesterics these lines were interpreted[26] as the periodic distribution of χ-lines (i.e., $\pm\pi$ twist disclinations) in the distance of a half-pitch of cholesteric helix.

At zero external field the repulsion of disclinations from the surface is balanced by the increase of energy necessary to unwind the helix of Sm C* which leads to the equilibrium distance of disclinations d from the surface. With thick samples this distance does not depend on the sample thickness. With samples of the thickness 2 h lower than $p_0/2\alpha$ the completely unwound structure corresponds to the stable state.

The simplified model presented in Part 4 describes qualitatively the field induced transition from Sm C* to Sm C phase in helical Sm C* sample with twist disclinations. The behavior of the sample depends on the original alignment in the surface layers and on the direction of the field:

1) For $\phi_0 = 0$ and $P_sE_z > 0$ or ($\phi_0 = \pi$, $P_sE_z < 0$) and when E_z reaches the critical value E_z^0 the induced Sm C* $\rightarrow$ Sm C transition occurs by means of mutual annihilation of opposite twist disclinations (see Part 4.3). The critical field E_z^0 is probably lower than that given in Ref. 1 as $E_c \approx \pi^4B_3/4p_0\mathrm{P}$ (P is the polarization). In our model the approximation is used, that the $\pm 2\pi$ twist disclinations are infinite so that they come together

being parallel and annihilate each other simultaneously along the whole length. In reality, however, the pair of disclinations forms a long loop which disappears by shortening its length. Long segments of the loop are shortened faster which is seen as the shortening of lines (Figures 1b, c). In this process the self energy of loop is reduced more rapidly.

2) For $\phi_0 = 0$ and $P_sE_z < 0$ (or $\phi_0 = \pi$, $P_sE_z > 0$) the disclinations move to the glass plates as it is seen from the Eq. (19) but this movement leads to the increase of the energy F (Eq. (14)). To decrease the energy a new molecular orientation $\phi_0 = \pi$ (or $\phi_0 = 0$) forms in the surface layers. The reorientation is associated with the shift of all disclinations by $p_0/2$ in the x-direction. The new orientation probably arises in a form of nuclei, which spread through the whole unwound surface layer. During this process the disclinations move. When the shift is completed and the orientation of molecules is changed from $\phi_0 = 0$ to $\phi_0 = \pi$ the disclination comes together as described in Part 4.3. The movement of disclinations by $p_0/2$ parallel to the glass plates is not experimentally confirmed.

The process of molecular reorientation from $\phi_0 = 0$ to $\phi_0 = \pi$ just described can be the cause of a dielectric hysteresis in Sm C* samples with helical structure.

These results, though obtained under simplifying conditions, qualitatively describe the Sm C* → Sm C transition which takes place in d.c. electric fields.

Theoretical approaches[14,16] which treated the unwinding of the ideal Sm C* structure by electric field in infinite sample gave continuous increase of p_0 to infinity if E_z increases to a critical field. This process does not take place in unwinding of Sm C* structure by d.c. field in real planar samples where the linear defects play an essential role.

The critical field $E_z^c = W_s/hP_s$ to change the orientation of molecules in the unwound sample depends principally on the surface anchoring energy W_s and not on the elastic constant B_3. The dependence of E_z^c on the sample thickness $2h$ is of the Fréedericksz type. It is necessary to have in mind that with unwound samples the formation and the growth of nuclei of a new orientation probably determine the value of switching field and it is also responsible for hysteresis similarly as in the switching of solid ferroelectrics. When hysteresis loop is observed in a.c. fields it is probable that the switching between two unwound orientations proceeds by means of nucleating a new orientation and not via helical structure.

As noted before, dechiralization lines are the consequence of Sm C* helical structure in samples with planar anchoring. However, as real defects they interact with the surfaces or other defects as e.g. focal conics.[28] This interaction is probably the reason why the distance between lines does not change in the x-direction (see Figure 5) under external influences. So the lines keep the pitch of Sm C* helix unchanged in d.c. electric field up to E_z^o and also when the temperature is changed.

In a low a.c. field the dechiralization lines oscilate in z-direction as described by Eq. (19), which is connected with changes of dipole moment of the sample. This process could be responsible for the low frequency contribution to the dielectric permittivity[12] which has been unexplained up to now.

The tendency of the DOBAMBC planar rather thick samples to stay in metastable unwound state without electric field implies the conclusion that the energy obtained by restoring the helical structure is comparable with the energy connected with the creation of dechiralization lines which are a necessary consequence of the helical structure.

Acknowledgment

The authors are indebted to Prof. R. Blinc and to the members of his group for supplying DOBAMBC liquid crystal.

References

1. R. B. Meyer, L. Liébert, L. Strzelecki, and P. Keller, *J. Physique Lett.*, **36**, L-69 (1975).
2. B. I. Ostrovski, A. Z. Rabinovich, A. S. Sonin, D. A. Strukov, and N. I. Chernova, *Pisma v Zh. Eksp. i Teor. Fiziki*, **25**, 80 (1977).
3. J. Hoffman, W. Kuczinski, and J. Malecki, *Mol. Cryst. Liquid Cryst.*, **44**, 287 (1978).
4. K. Yoshino, T. Uemoto, and Y. Inuishi, *Japan J. Appl. Phys.*, **16**, 571 (1977).
5. P. Martinot-Lagarde, *J. Physique Colloq.*, **37**, C-129 (1976).
6. L. K. Vistin, S. P. Chumakov, and Z. B. Rajabova, *Advances in Liquid Crystal Research and Applications* (Editor L. Bata, Pergamon Press, Oxford–Akadémiai Kiadó, Budapest 1980), p. 483.
7. P. Martinot-Lagarde, R. Duke, and G. Durand, *Mol. Cryst. Liquid Cryst.*, **15**, 249 (1981).
8. K. Kondo, A. Fukuda, and E. Kuze, *Jap. Journ. Appl. Phys.*, **20**, 1779 (1981).
9. M. Brunet and C. Williams, *Ann. Physique* **3**, 237, (1978).
10. L. Bourdon, Thése de 3ᵉ Cycle, Orsay (1980).
11. A. Perez, Thése de 3ᵉ Cycle, Montpellier (1980).
12. A. Levstik and C. Filipič, 4th Liquid Cryst. Conf. Soc. Countries, Tbilisi 1981.
13. S. A. Pikin and V. L. Indenbom, *Uspechi Fiz. nauk*, **125**, 251 (1978).
14. V. E. Dimitrienko, V. A. Belyakov, *Zh. Eksp. i Teor. Fiziki*, **78**, 1569 (1980).
15. P. Martinot-Lagarde, *Mol. Cryst. Liquid Cryst.*, **66**, 381/61 (1981).
16. O. Hudák, *J. Physique*, in print.
17. B. I. Ostrovski, S. A. Pikin, and V. G. Chigrinov, *Zh. Eksp. i Teor. Fiziki*, **77**, 1615 (1979).
18. M. Glogarová, L. Lejček, J. Pavel, V. Janovec, and J. Fousek, *Czech. J. Phys.*, **B32**, 943 (1982).
19. N. A. Clark and S. T. Lagerwall, *Appl. Phys. Lett.*, **36**, 899 (1980).
20. A. Rapini, *J. Physique*, **33**, 237 (1972).
21. Y. Bouligand and M. Kléman, *J. Physique*, **40**, 79 (1979).

22. R. Blinc and B. Žekš, *Phys. Rev.*, **A18**, 740 (1978).
23. M. Kléman, Points, lignes, parois dans les fluides anisotropes et les solides cristallins, Vol. 1 (Les Éditions de Physique 1977)
24. M. Kléman, *J. Physique*, **35**, 595 (1974).
25. L. Bourdon, J. Sommeria, and M. Kléman, *J. Physique*, **43**, 77 (1982).
26. P. Cladis and M. Kléman, *Mol. Cryst. Liquid Cryst.*, **16**, 1 (1972).
27. G. Leibbrandt, *Phys. Rev.*, **B15**, 3353 (1977).
28. A. Perez, M. Brunet, and O. Parodi, *J. Physique*, **42**, 1559 (1981).